

Aquaculture

September 2014, Volume 433 Pages 450-457

<http://dx.doi.org/10.1016/j.aquaculture.2014.07.006><http://archimer.ifremer.fr/doc/00202/31287/>

© 2014 Elsevier B.V. All rights reserved.

Achimer<http://archimer.ifremer.fr>

Influence of suspended mussel lines on sediment erosion and resuspension in Lagune de la Grande Entrée, Îles-de-la-Madeleine, Québec, Canada

Walker Tony R. ^{1,*}, Grant Jon ¹, Weise Andréa M. ², Mckindsey Christopher W. ^{2,3}, Callier Myriam ^{2,3,4},
Richard Marion ^{2,3,5}

¹ Dalhousie University, Department of Oceanography, Halifax, NS, Canada

² Fisheries and Oceans Canada, Maurice Lamontagne Institute, Environmental Sciences Division, 850 route de la mer, Mont Joli, QC, Canada

³ Institut des Sciences de la Mer, Université du Québec à Rimouski, 310 allée des Ursulines, Rimouski, QC, Canada

⁴ Institut Français de Recherche pour l'Exploitation de la Mer (IFREMER), Centre Méditerranée, Département des Ressources Biologiques et Environnement, Laboratoire Aquaculture Languedoc Roussillon, UMR 5119 ECOSYM, Chemin de Maguelone, Station de Palavas, 34250 Palavas-les-Flots, France

⁵ Institut Français de Recherche pour l'Exploitation de la Mer (IFREMER), Département Océanographie et Dynamique des Écosystèmes, Laboratoire Environnement Ressources du Languedoc Roussillon, Station de Sète — Avenue Jean Monnet, 34203 Sète, Cedex, France

* Corresponding author : Tony R. Walker, email address : tonyrobertwalker@gmail.com

Abstract :

Downward fluxes of organically rich biodeposits under suspended mussel lines can cause benthic impacts such as changes in benthic community structure or microbial mat production. Quantifying sediment erosion in these coastal ecosystems is important for understanding how fluxes of organic matter and mussel biodeposits contribute to benthic–pelagic coupling. Critical shear velocity (u^* crit), erosion rates and particle size distributions of resuspended sediment were measured at four stations distributed along a transect perpendicular to a mussel farm in Lagune de la Grande Entrée, Îles-de-la-Madeleine (Quebec, Canada). Stations were selected underneath the outer-most mussel line (0 m) and at distances of 15, 30 m and at a reference station (500 m) further along the transect. Shear velocity was measured using a calibrated portable Particle Erosion Simulator, also referred to as the BEAST (Benthic Environmental Assessment Sediment Tool). Undisturbed sediment cores obtained by divers were exposed to shear stress to compare differences between stations. Erosion sequences indicated no significant differences in u^* crit between stations, but there were significant differences in erosion rates beneath mussel lines compared to other stations. Erosion rates were the highest in cores from beneath mussel lines, but paradoxically had the lowest u^* crit. Mean erosion rates at u^* crit varied between 25 and

47 g m⁻² min⁻¹ and critical erosion thresholds varied between 1.58 and 1.73 cm s⁻¹, which compare with intensive mussel culture sites elsewhere in eastern Canada. Significant differences existed in biotic and abiotic properties of sediments which could explain variation in maximum erosion rates within and between stations. Particle sizes measured by videography of resuspended sediment at different shear velocities ranged from 0.2 to 3.0 mm. Quantifying sediment erosion from intact marine sediments helps to improve our mechanistic understanding of these processes, and the BEAST further contributes to predictive capability in benthic–pelagic coupling modeling.

Highlights

► An erosion device was used to quantify sediment near cultured mussels. ► Erosion rates were significantly higher beneath mussel lines. ► Critical shear velocities compared to other studies in eastern Canada ► The BEAST contributes to our understanding of benthic–pelagic coupling.

Keywords : Sediment erosion, Shear velocity, Resuspension, Biodeposits, Particle size, *Mytilus edulis*

1. Introduction

Quantification of sediment erosion around coastal aquaculture operations is essential for understanding fluxes of organic rich particulate matter. Sedimentation, sinking rates and dispersion of organic and inorganic particles (comprising of phytoplankton, sediment, detritus, fecal pellets or resuspended aggregates), is dependent on particle diameter and density, and are highly variable in coastal water columns (Andersen et al., 2002; Miller et al., 2002; Nickell et al., 2003; Giles and Pilditch, 2004). Sedimentation is further compounded by filter-feeding bivalves which play an important role in coastal ecosystems through their influence on benthic-pelagic coupling and nutrient cycling (Christensen et al., 2003). Filter-feeding bivalves repack fine suspended material into larger organic rich biodeposits (feces and pseudofeces) that sink more rapidly than their constituents, increasing fluxes of organic matter to the benthos, depending on water depth, currents and resuspension (Chamberlain et al., 2001). While dynamics of mussel biodeposition (resuspension and disaggregation) is poorly quantified, enhanced sedimentation under mussel culture is well documented (e.g., Hatcher et al., 1994; Callier et al., 2006).

1
2
3
4 69 Bottom sediment resuspension is affected by biostabilization, porosity, organic
5
6 70 content, grain size, and bioturbation (Miller et al., 2002; Nickell et al., 2003; Giles and
7
8
9 71 Pilditch, 2004; Walker and Grant, 2009). Quantifying sediment resuspension is important
10
11 72 for understanding sediment erosion thresholds (critical shear velocity, u_{*crit}) and fluxes
12
13
14 73 generated by currents or waves becomes an important predictive tool in coastal
15
16 74 ecosystem management. Quantifying sediment transport is possible when erosion
17
18
19 75 thresholds are known, although few calibrated data exist for sediment entrainment rates
20
21 76 (Tolhurst et al., 2000; Grant et al., 2013), especially those influenced by mussel
22
23
24 77 biodeposits or microbial mats (Walker and Grant, 2009). Sediment stability (defined as
25
26 78 increased erosion threshold) is often associated with biostabilizing microbial mats,
27
28
29 79 including diatoms and/or bacteria which can physically bind cohesive and non-cohesive
30
31 80 sediment particles via the excretion of extracellular polymeric substances (Grant et al.,
32
33
34 81 1986; Grant and Gust, 1987; Tolhurst et al., 2002). Alternatively, bioturbation can
35
36 82 destabilize sediments by increasing porosity or by grazing on stabilizing organisms
37
38
39 83 (Gerdol and Hughes, 1994). Sediment erosion thresholds are therefore difficult to predict,
40
41 84 due to varying biotic and abiotic influences. Moreover, erosion thresholds are difficult to
42
43 85 measure for undisturbed sediments, requiring substantial effort using laboratory or field
44
45
46 86 flume quantification (Widdows et al., 1998).

47
48 87 Downward fluxes of organic biodeposits under suspended mussel culture operations
49
50
51 88 has been reported to have local adverse benthic impacts, decreasing biodiversity and
52
53 89 increasing sulfate reduction leading to anaerobic conditions (see review by McKindsey et
54
55
56 90 al., 2011). Whilst some modeling studies have considered erosion and dispersion around
57
58 91 mussel aquaculture sites (Giles et al., 2009; Wiese et al., 2009), combined field
59
60
61
62
63
64
65

1
2
3
4 92 measurements of sediment erosion rates from suspension-feeding bivalves has rarely
5
6
7 93 been investigated (Widdows et al., 1998; Miller et al., 2002; Giles and Pilditch, 2004;
8
9 94 Walker and Grant, 2009). Recent studies associated with mussel aquaculture in Lagune
10
11 95 de la Grande Entrée (LGE) have documented benthic impacts associated with
12
13
14 96 biodeposition, including nutrient and particle fluxes (Callier et al., 2006, 2009; Richard et
15
16 97 al., 2006, 2007a, 2007b). Ecosystem models of aquaculture carrying capacity on the
17
18 98 basis of mussel grazing have also been conducted there (Grant et al., 2007; Filgueira et
19
20 99 al., 2012). However, the fate of biodeposits through dispersion and resuspension events
21
22
23 100 remains unclear in LGE (Callier et al., 2006; Weise et al., 2009). This is especially
24
25
26 101 important if benthic microalgae are resuspended as an additional mussel food source
27
28
29 102 (Frechette and Grant, 1991).

30
31 103 We re-designed and calibrated a portable erosion chamber called the 'Benthic
32
33 104 Erosion Assessment Sediment Tool' (BEAST) (Grant et al., 2013) to measure erosion in
34
35
36 105 undisturbed sediment cores in an attempt to field verify biodeposit dispersion model
37
38 106 predictions in LGE. The following objectives were undertaken: (1) quantify erosion
39
40
41 107 thresholds, erosion rates, and resuspended particle size distributions along a SW transect
42
43 108 perpendicular to a mussel line in the direction of main current flow; (2) determine
44
45 109 sediment organic quality; and (3) compare erosion features to a separate study by Callier
46
47
48 110 et al. (2006) who measured downward fluxes of biodeposits and spatial extent of
49
50
51 111 dispersion investigated via sediment traps located along the same transect.

52
53 112

54 55 113 **2. Methods**

56 57 58 114 *2.1. Study site*

59
60
61
62
63
64
65

1
2
3
4 115 This study was conducted below and adjacent to a mussel farm in LGE, Îles-de-la-
5
6 116 Madeleine, Quebec, in August 2004. Îles-de-la-Madeleine are in the Gulf of St. Lawrence
7
8
9 117 in eastern Canada, with LGE (58 km²) located in the northeast of the largest island (47°
10
11 118 37' N, 61° 31' W). Mean currents are weak (<5 cm s⁻¹) occasionally increasing to 10 cm
12
13 119 s⁻¹ during strong wind events, resulting in a well-mixed water column (Koutitonsky et al.,
14
15 120 2002). A deep navigation channel (8 m) separates LGE into a shallow (1-3 m) sandy area
16
17 121 to the west and a deeper (5-7 m) muddy basin to the east where the mussel farm is located
18
19 122 (Fig. 1). Blue mussels, *Mytilus edulis* L. are cultured using longlines with continuous
20
21 123 socking looping between floats and the farm has operated since the 1980s, currently
22
23 124 producing 180 t yr⁻¹ in a farm area of 2.5 km² (Weise et al., 2009).
24
25
26
27
28
29
30

125

126 2.3. Sediment sampling stations

127 Triplicate intact sediment samples were collected in Plexiglas™ cores (11.2 cm I.D.) by
128 SCUBA divers for erosion experiments and particle size distribution from stations along
129 a SW transect perpendicular to a mussel line along the direction of main current flow
130 (i.e., underneath a mussel line to a reference station). Sampling stations were located 0,
131 15 and 30 m from the mussel line. A reference station was selected at a sandy site located
132 500 m further along the transect (Fig. 1). Three additional sediment cores were collected
133 from each station for determination of sediment physical properties, using sub-cores over
134 the 0-1 cm depth horizon with truncated 5 mL plastic syringes for measurement of grain
135 size, percent organic matter (%OM), percent total organic carbon (%TOC) and C:N
136 ratios.

137

1
2
3
4 138 *2.4. Sediment properties*

5
6
7 139 Sub-samples were stored at -20C in pre-weighed plastic scintillation vials until analysis.

8
9 140 Triplicate thawed samples were wet sieved with tap water through 63-2000 μm sieves.

10
11 141 Sub-samples of $<63 \mu\text{m}$ suspended sediment were collected and filtered through GF/F

12
13
14 142 filters for analysis of %OM. For %OM, filter residues and sediments were oven dried at

15
16 143 60°C for 3 d to constant weight, followed by ashing in a furnace oven at 520°C for 24 h

17
18 144 before re-weighing. Sediment texture distribution was determined using GRADISTAT

19
20 145 (Blott and Pye, 2001). Sediments were analyzed for C:N ratios using a CHN elemental

21
22 146 analyzer (Perkin-Elmer 2400) (Walker, 2005).

23
24
25
26 147

27
28 148 *2.5. Sediment erosion thresholds and erosion rates*

29
30 149 Sediment erosion thresholds and erosion rates were determined on triplicate cores from

31
32 150 each station using the BEAST with methods that have been reported elsewhere in greater

33
34 151 detail (Walker et al., 2008; Walker and Grant, 2009; Grant et al., 2013). Briefly, cores

35
36 152 were filled with approximately 1 L of seawater overlying a 30 cm sediment column and

37
38 153 stored in a dark water bath (10°C) to equilibrate before erosion was performed. The

39
40 154 plunger disc was inserted into the core liner, and oscillation imposed for 2 min. intervals

41
42 155 at equivalent shear velocities of 0.9-2.6 cm s^{-1} . Onset of sediment erosion was detected

43
44 156 via turbidity and digital imaging. Initial particle movement is detected as erosion of flocs,

45
46 157 while the sediment surface remains intact. Critical shear velocity is defined as a more

47
48 158 generalized failure of the bed. We have used these categories previously (Grant et al.,

49
50 159 2013), finding them to be more applicable to our BEAST erosion sequences than the

51
52 160 Type I and II terms classically used (Tolhurst et al., 2000).

53
54
55
56
57
58
59
60
61
62
63
64
65

1
2
3
4 161 Turbidity in erosion chamber was monitored using % transmission as a proxy for
5
6 162 sediment concentration with an *in situ* fiber-optic spectrophotometer (Brinkmann PC 800
7
8
9 163 colorimeter, 670 nm). The fiber-optic probe was zeroed with filtered seawater and
10
11 164 calibrated using thawed frozen sediment samples covering a range of concentrations from
12
13
14 165 all stations. Sediment slurries were filtered through GF/F to determine suspended
15
16 166 particulate matter (SPM) concentrations.

17
18
19 167 Sequences of sediment erosion and erosion activity at the sediment bed were
20
21 168 recorded visually using a mini-DV camcorder (Canon ZR45 MC) and analyzed following
22
23 169 protocols from our previous studies (Walker et al., 2008). Digital still images were
24
25
26 170 obtained at 1 min. intervals using video capture software (Pinnacle Studio version 8,
27
28 171 Pinnacle systems). Particle size analysis of images was determined with SigmaScan Pro
29
30 172 version 5 (SPSS Inc.) image analysis software. Particles could only be discriminated at
31
32
33 173 lower shear velocities before SPM concentrations became too turbid. Minimum particle
34
35 174 sizes measured using estimated spherical diameter (ESD) was 200 μm .

36
37
38 175 Erosion rates were calculated according to Walker and Grant (2009). The
39
40
41 176 spectrophotometer gave linear responses to SPM concentrations of sandy sediments at all
42
43 177 stations covering concentrations from 0-7700 mg L^{-1} , so that each % transmission unit
44
45
46 178 represented a specific SPM concentration. Erosion rates were calculated for each time
47
48 179 interval based on this linear relationship with respect to sediment core surface area (98
49
50 180 cm^2).

51
52
53 181

54
55 182 *2.7. Statistical analysis*
56
57
58
59
60
61
62
63
64
65

1
2
3
4 183 Significant differences were determined using Minitab to perform one-way analysis of
5
6 184 variance (ANOVA) followed by Tukey's test at the $P < 0.05$ level (unless indicated
7
8
9 185 otherwise).

10
11 186

12 13 14 187 **3. Results**

15 16 188 *1.1. Sediment properties*

17
18
19 189 Sediment grain size composition and significance tests for %TOC, %OM and C:N ratios
20
21 190 are shown in Fig. 2. Sediments were comprised of silty sand at 0 m or fine sand at
22
23 191 remaining stations. Median grain sizes (D_{50}) at 0 m were 90 μm , with similar slightly
24
25 192 coarser sizes at 15 and 30m, increasing to 180 μm at 500 m. Percent TOC and %OM
26
27 193 varied between stations with lowest values measured at 500 m. This was expected of the
28
29 194 coarser sediment found in the far field. However, the 0m farm sediments were finest, yet
30
31 195 lower in %OC than the more distant farm sites. The 15 and 30m sediments were not
32
33 196 significantly different in organic or carbon content. Sediment C:N ratios were 7-8 at 15,
34
35 197 30, and 500m, but significantly higher at 0m with a values of 12. This may reflect more
36
37 198 degraded sedimentary organic material arising from mussel feces.

38
39
40
41
42
43 199

44 45 200 *3.2. Erosion experiments*

46
47
48 201 Observations of erosion sequences show consistent behaviour of the three variables (Fig.
49
50 202 3). Shear stress is applied in consistent linear manner. Turbidity remains constant or
51
52 203 displays a slow increase as flocs are resuspended until the initiation of more general
53
54 204 erosion, and then shows a steep increase (declining % transmission). Erosion rate
55
56
57 205 provides an instantaneous measure of sediment dynamics that remains at a low level until
58
59
60
61
62
63
64
65

1
2
3
4 206 the onset of general erosion when it displays a marked increase. The shapes of these
5
6 207 curves are used to distinguish important differences between stations. Specifically,
7
8
9 208 turbidity curves in cores from beneath mussel lines, experienced sharp transitions to
10
11 209 erosion once protective organic rich carpets were disrupted at this station (Fig. 3). This
12
13
14 210 was in contrast to other stations, where transitions to erosion were more gradual,
15
16 211 probably due to larger grain sizes and the absence of mats. Critical shear velocity (u^*_{crit})
17
18 212 was reached between 1.58-1.73 cm s^{-1} at all stations. Mean erosion rates at u^*_{crit} varied
19
20 213 between 25-47 $\text{g m}^{-2} \text{min}^{-1}$ at 30 m and 0 m, respectively.
21
22

23
24 214
25
26 215 The behaviour of both turbidity and erosion rate are variable in the chamber experiments,
27
28 216 and few consistent differences between stations can be observed. In some cases, an
29
30
31 217 increase in turbidity occurred well before the general erosion threshold, indicating that
32
33 218 the accumulation of surface flocs accounts for substantial resuspension. As expected, the
34
35
36 219 onset of general erosion occurs at the peak of erosion rate, and after a rapid increase in
37
38 220 this rate. The only consistent spatial difference is that in cores from the mussel farm,
39
40
41 221 initial floc movement began at a lower speed than at reference sites. Otherwise, metrics
42
43 222 such as the erosion threshold and the erosion rate at this threshold are variable enough to
44
45
46 223 obscure spatial differences.

47
48 224 Cores from 0 m appeared to have a shallow light brown oxidized layer which
49
50 225 penetrated <1.5 cm, although according to Callier et al. (2008) these sediments were
51
52
53 226 largely anoxic up to a depth of 10 cm below the surface. Before onset of erosion the
54
55 227 water column remained clear, but with increasing shear stress, larger particles (>0.4 mm)
56
57
58 228 began lifting. The first phase of erosion was observed when turbidity began to increase at
59
60
61
62
63
64
65

1
2
3
4 229 1.40 cm s⁻¹. As further stress was applied, the bed failed and the second phase of erosion
5
6 230 was observed ($u^*_{crit} = 1.58 \text{ cm s}^{-1}$), with the suspension becoming fully turbid. Shear
7
8
9 231 stress at u^*_{crit} was sufficient to lift larger particles (upto 2 mm) and maintain them in
10
11 232 suspension.

13
14 233 Cores from 15 m contained deeper light brown surface layers between 0.5-2 cm.
15
16 234 The second phase of erosion, occurred at u^*_{crit} of 1.73 cm s⁻¹ and shear stress was
17
18 235 sufficient to lift particles between 0.2-1 mm. Cores from 30 and 500 m stations contained
19
20
21 236 a shallow light brown surface layer between 0.6-1 cm deep and the second phase of
22
23 237 erosion occurred at u^*_{crit} of 1.67 cm s⁻¹ and 1.72 cm s⁻¹, respectively with particles
24
25
26 238 between 0.2-3 mm.

27
28 239 Decreasing % transmission values had tight linear relationships with SPM
29
30 240 concentration measured by filtration and gravimetry ($R^2 = 0.93-0.99$), corresponding to
31
32 241 mean SPM concentrations of between 2931 to 7763 mg L⁻¹ (Fig. 4a). Mean erosion rates
33
34 242 were recorded up to $47 \pm 2.9 \text{ g m}^{-2} \text{ min}^{-1}$ at 0 m and only $25 \pm 2.5 \text{ g m}^{-2} \text{ min}^{-1}$ at 30 m from
35
36 243 the mussel line and were significantly different ($P < 0.01$) (Fig. 4b). There were no
37
38 244 obvious relationships between critical shear stress and erosion rates across stations ($R^2 =$
39
40 245 0.29) (Fig. 4c). Frequency of resuspended particle sizes, with increasing shear velocity,
41
42 246 ranged from 0.1-3.0 mm for all stations and for all erosion thresholds (Fig. 5). Image
43
44 247 analysis of particles sizes became difficult $>u^*$ of 1.7 cm s⁻¹, due to increasing turbidity.
45
46 248 Particles $<200 \mu\text{m}$ were below levels of detection for this method and are not shown.
47
48
49 249 Overall, there appears to be subtle differences in particle size distributions across stations,
50
51 250 with more particles resuspended at lower shear velocities at 0 m compared to 500 m.
52
53
54
55
56
57
58
59
60
61
62
63
64
65

251

252 4. Discussion

253 One of the primary impacts of mussel culture is enhanced biodeposition of fecal and
254 pseudofecal material (Cranford et al., 2009). Many studies have documented
255 environmental effects due to this increased sedimentation including impacts associated
256 with eutrophication, e.g., sediment hypoxia, increased sulfate reduction, and greater
257 effluxes of ammonium (Danovaro et al., 2004; Hartstein and Rowden, 2004; Callier et al.,
258 2007, 2008; Richard et al., 2007a, 2007b; McKindsey et al., 2011). Among the resultant
259 biotic responses to organic loading are the development of microbial mats, and decline in
260 benthic invertebrate biodiversity due to their sensitivity to sulfide concentrations (Pearson
261 and Rosenberg, 1978; Hatcher et al., 1994; Chamberlain et al., 2001).

262 Several studies have shown that increasing biodeposition from bivalve culture
263 may lead to changes in sediment composition, resulting in muddy, anaerobic sediments
264 (e.g., Hatcher et al., 1994). In our study, the finest sediment was found at the mussel
265 lines, mirroring size fractions reported by Callier et al. (2006, 2008). Sediment at the
266 longlines also had the highest C:N suggesting that the biodeposits are degraded from
267 grazing and digestion. Callier et al. (2008) did not report any significant difference
268 between other sediment characteristics (including %OM) or benthic communities along
269 the same transect. Taken together these studies and the present work suggest that the
270 LGE farm had little effect on the local environment. The lack of localized impacts in
271 LGE was perhaps influenced by wind induced resuspension in this shallow water site
272 (Koutitonsky et al., 2002).

273 Critical erosion thresholds of sediments at all stations occurred when shear
274 velocities reached between 1.58-1.73 cm s⁻¹, which compare favorably with field

1
2
3
4 275 measurements made at intensive mussel culture sites in Prince Edward Island, Canada
5
6 276 (Walker and Grant, 2009). Analysis of sediment erosion sequences indicated there were
7
8
9 277 no significant differences in sediment u^*_{crit} between stations and there was as much inter-
10
11 278 as intra-station variation, although the limited replicates used in this study probably
12
13 279 highlighted the relatively high intra-station variation. More studies using additional cores
14
15 280 to perform erosion sequences would likely decrease the intra-treatment variability of our
16
17 281 erosion thresholds and may potentially highlight significant differences along the
18
19 282 transect. There were however significantly higher erosion rates beneath mussel lines (47
20
21 283 $\text{g m}^{-2} \text{min}^{-1}$), where fluxes of organic matter to sediments were high due to increased
22
23 284 biodeposition, compared to 30 m ($25 \text{ g m}^{-2} \text{min}^{-1}$). A simple explanation is that there is
24
25 285 similar fine material in a background of sand at each site. This produces a similar
26
27 286 threshold for erosion based on a visual criterion or change in turbidity. However, the
28
29 287 erosion rate is greater at the longlines, because there is more of the fine material available
30
31 288 to erode. If shear velocity is estimated as 5% of free stream (Gordon et al., 2004), then
32
33 289 even the higher range of currents measured in the vicinity of the farm are below critical
34
35 290 shear velocity.

36
37
38 291 Our erosion sequences clearly show two phases of erosion, an initial phase
39
40 292 (surficial) and a second phase (critical erosion). According to Tolhurst et al. (2000)
41
42 293 cohesive sediments erode in several phases, as a function of depth of the eroded layer.
43
44 294 We demarcated the distinction between phases of erosion on the basis of surficial layer
45
46 295 events, where the first phase of erosion (i.e., flocs, biofilms, surface mm of sediment) was
47
48 296 compared to the second phase of erosion (i.e., failure of sediment surface to cm-scale
49
50 297 depths and a sharp increase in turbidity) (Grant et al., 2013).
51
52
53
54
55
56
57
58
59
60
61
62
63
64
65

1
2
3
4 298 Initially, in all cores, except for those collected beneath mussel lines (0 m), there
5
6 299 was little or no change in turbidity, with only a few small particles eroding from the
7
8
9 300 surface (first phase of erosion). However as turbidity began to increase, erosion rates
10
11 301 increased dramatically until a second phase of erosion was achieved whereby further
12
13
14 302 increases in shear stress did not appear to increase erosion rates. Although sediment
15
16 303 concentration and particle size maybe difficult to correlate at high shear velocities (due to
17
18 304 poor visibility in cores), they are both dependant on turbulent shear (Walker et al., 2008).
19
20
21 305 At low shear velocities in erosion sequences using sediment cores collected from beneath
22
23 306 suspended mussel lines it appeared that larger aggregates were resuspended first (Fig. 5).
24
25
26 307 For example, in our recent studies on microbial mats, sediments which were initially
27
28 308 biostabilized against erosion due to an 'armoring' effect, the onset of erosion was abrupt
29
30
31 309 once these mats failed, resulting in the resuspension of large mat fragments (Walker and
32
33 310 Grant, 2009).

34
35
36 311 Much of the feces biodeposition, from mussel culture may have become
37
38 312 incorporated into these sediments and the method used here for sediment grain size
39
40 313 analysis may have resulted in the destruction of these bio-aggregates. This may have
41
42 314 underestimated the binding effects of the microbial mats and may therefore, not correlate
43
44 315 well with sediment erodibility, particularly for sediments beneath mussel lines which had
45
46 316 the highest erosion rates. Studies by Fugate and Friedrichs (2003) noted that biological
47
48 317 aggregations initially resisted turbulent breakup in sediment erosion studies in
49
50
51 318 Chesapeake Bay, but Paterson (1989), found that sediments underlying biofilms (once
52
53 319 exposed), were more easily eroded than the biostabilized layer itself. A similar response
54
55
56 320 in sediment stability was observed by Walker and Grant (2009) around mussel culture
57
58
59
60
61
62
63
64
65

1
2
3
4 321 sites in Tracadie Bay, where mean erosion thresholds of 1.74 cm s^{-1} and erosion rates of
5
6 322 $47 \text{ g m}^{-2} \text{ min}^{-1}$ were recorded. These results compare favorably with erosion rates and
7
8
9 323 thresholds reported in this study, as erosion experiments on cores containing large areas
10
11 324 of eelgrass, *Zostera marina* initially resisted erosion, but when turbulent breakup did
12
13
14 325 occur, large fragments above the sediment bed were observed.

15
16 326 Erosion rate calculations respond to small changes in turbidity at each time step
17
18 327 and are a sensitive indicator of instantaneous resuspension. As the first phase of erosion
19
20
21 328 began, a steep rise in erosion rate was observed. With increased stress, more scouring of
22
23
24 329 unconsolidated material occurred and during the second phase of erosion, the rate began to
25
26 330 decrease as the bed eroded to more consolidated sediments yielding fewer and larger
27
28 331 particles. These observations reiterate previous studies which demonstrate that there are
29
30
31 332 multiple erosion thresholds, dependent on sediment texture and the vertical distribution of
32
33 333 shear strength (Tolhurst et al., 2000).

34
35
36 334 Erosion rates around mussel culture sites in this study were higher than those
37
38 335 reported by Giles and Pilditch (2004), that found organic rich biodeposits from mussels
39
40
41 336 were easily eroded at thresholds $<1 \text{ cm s}^{-1}$. Again, this was probably due in part to
42
43 337 biostabilization of microbial mats, the presence of eelgrass and the textural properties of
44
45 338 sediments beneath mussel lines in LGE. Normally in natural sediments fecal material
46
47
48 339 reduces sediment stability (Andersen et al., 2002), but in this study biodeposits probably
49
50 340 contributed to microbial mat biomass.

51
52
53 341 Several physical and biological properties of the sediment surface were measured
54
55 342 in order to determine a suitable quantitative predictor of the erodibility of sediment (e.g.,
56
57
58 343 grain size, %OM content, %TOC and C:N ratios). There were also other contributions to
59
60
61
62
63
64
65

1
2
3
4 344 organic enrichment in LGE, such as the presence of large amounts of detritus (e.g.,
5
6 345 eelgrass) and microbial mats revealed from diver observations and evidenced in several
7
8 346 core samples. The accumulation of fine particles in the sediment at these sites may be
9
10 347 influenced by limited tidal exchange, removal of biodeposits by feeding mussels during
11
12 348 wind-induced resuspension events, and subsequent biostabilization of the fine fraction at
13
14 349 the sediment-water interface by microbial mats, and the construction of a navigation
15
16 350 channel in the 1980's which probably changed the hydrodynamics of the lagoon. The
17
18 351 physical characteristics of the sediments at these stations, and others along the transect in
19
20 352 LGE have previously been described by (Callier et al., 2006, 2007), who reported no
21
22 353 difference in sediment %OM between 0 and 15 m from the mussel line. Also they found
23
24 354 no difference in the depth of the sediment oxic layer between 0 and 15 m from mussel
25
26 355 line, where sediments were reduced and blackened with a sulfide layer, however, the 30
27
28 356 m station was more oxidized. There was also no difference in abundance of infauna, wet
29
30 357 weight biomass and diversity of species between the three stations at 0, 15 and 30 m
31
32 358 (Callier et al., 2007).

33
34
35
36
37
38
39
40
41 359 Callier et al. (2006) reported that measured deposition of mussel biodeposits were
42
43 360 fairly localized along the transect in LGE, albeit with some inter-annual variation, and
44
45 361 was in broad agreement with modeled biodeposit settling rates by Weise et al. (2009).
46
47 362 However negative benthic impacts were more diffuse along the same transect. The
48
49 363 amount of organic enrichment along the transect in this study was fairly uniform except
50
51 364 at the reference station, which may partly explain the lack of significant differences
52
53 365 observed in erosion sequences between stations. However, the amount of %TOC and
54
55 366 %OM was highest at 30 m from the mussel line, suggesting that dispersal via the
56
57
58
59
60
61
62
63
64
65

1
2
3
4 367 dominant current flow direction (with current velocities sometimes exceeding u^*_{crit} values
5
6 368 measured here), was responsible for transporting material. The lowest erosion thresholds
7
8
9 369 (but highest erosion rates), were recorded directly below the mussel line, where the
10
11 370 increased deposition of organically rich biodeposits may have already caused changes in
12
13 371 the sediment textural properties but not the benthic community structure (Callier et al.,
14
15 372 2006). This contrasts to the increases in grain size observed further along the transect,
16
17 373 where slightly higher erosion thresholds were observed.
18
19
20

21 374 Our work in modeling the role of resuspension in benthic-pelagic coupling is
22
23 375 limited by accurate estimates of erosion characteristics, whose prediction is often mired
24
25 376 in complex biophysical interactions (Grant et al., 2013; Walker et al., 2008). This is
26
27 377 particularly true of erosion studies with microbial mats where armoring is so important to
28
29 378 the erosion process close to mussel aquaculture sites (Walker and Grant, 2009). The use
30
31 379 of the BEAST as a proxy for quantifying sediment erosion demonstrates its practical
32
33 380 capability to provide quantitative field measurements of transport parameters from
34
35 381 undisturbed marine sediments to improve our mechanistic understanding of these
36
37 382 processes, and further contributes to predictive capability in modeling of benthic-pelagic
38
39 383 coupling. Future applications using this device could include environmental effects
40
41 384 monitoring to improve habitat and ecosystem management of potential changes in
42
43 385 benthic ecosystems near coastal aquaculture operations. More studies are required in
44
45 386 order to fully understand the effects of sediment erosion and resuspension from the
46
47 387 impacts of biodeposition from mussel aquaculture in these shallow coastal sites.
48
49
50
51
52
53
54

55 388

56
57
58 389 **Acknowledgements**
59
60
61
62
63
64
65

1
2
3
4 390 We thank MAPAQ and B. Hargrave for collaboration and C. Éloquin and associates for
5
6 391 permission to use their site. Funding was provided by Aquaculture Collaborative
7
8
9 392 Research and Development Program (ACRDP), Société de Développement de l'Industrie
10
11 393 Maricole (SODIM) and Fisheries and Oceans Canada. We thank B. Schofield and M.
12
13
14 394 Merrimen for fabrication of the BEAST which formed part of the equipment necessary
15
16 395 for the Canadian Arctic Shelves Exchange Study (CASES), a Research Network funded
17
18
19 396 by the Natural Sciences and Engineering Research Council of Canada (NSERC).
20
21 397

23 398 **References**

- 24
25
26 399 Andersen, T.J., Jensen, K.T., Lund-Hansen, L., Mouritsen, K.N., Pejrup, M., 2002.
27
28 400 Enhanced erodibility of fine-grained marine sediments by *Hydrobia ulvae*. J. Sea Res. 48,
29
30 401 51-58.
31
32
33 402 Blott, S.J., Pye, K., 2001. GRADISTAT: A grain size distribution and statistics package
34
35 403 for the analysis of unconsolidated sediments. Earth Surf. Process Landforms 26, 1237-
36
37 404 1248.
38
39
40 405 Callier, M.D., Weise, A.M., McKindsey, C.W., Desrosiers, G., 2006. Sedimentation rates
41
42 406 in a suspended mussel farm (Great-Entry Lagoon, Canada): biodeposit production and
43
44 407 dispersion. Mar. Ecol. Prog. Ser. 322, 129-141.
45
46
47 408 Callier, M.D., McKindsey, C.W., Desrosiers, G., 2007. Multi-scale spatial variations in
48
49 409 benthic sediment geochemistry and macrofaunal communities under a suspended mussel
50
51 410 culture. Mar. Ecol. Prog. Ser. 348, 103-115.
52
53
54
55
56
57
58
59
60
61
62
63
64
65

- 1
2
3
4 411 Callier, M.D., McKindsey, C.W., Desrosiers, G., 2008. Evaluation of indicators used to
5
6 412 detect mussel farm influence on the benthos: two case studies in the Magdalen Islands,
7
8 413 Eastern Canada. *Aquaculture* 278, 77-88.
9
10 414 Callier, M.D., Richard, M., McKindsey, C.W., Archambault, P., Desrosiers, G., 2009.
11
12 415 Responses of benthic macrofauna and biogeochemical fluxes to various levels of mussel
13
14 416 biodeposition: an in situ "benthocosm" experiment. *Mar. Pollut. Bull.* 58, 1544-1553.
15
16 417 Chamberlain, J., Fernandes, T.F., Read, P., Nickell, T.D., Davies, I.M., 2001. Impacts of
17
18 418 deposits from suspended mussel (*Mytilus edulis* L.) culture on the surrounding surficial
19
20 419 sediments. *ICES J. Mar. Sci.* 58, 411-416.
21
22 420 Christensen, P.B., Glud, R.N., Dalsgaard, T., Gillespie, P., 2003. Impacts of longline
23
24 421 mussel farming on oxygen and nitrogen dynamics and biological communities of coastal
25
26 422 sediments. *Aquaculture* 218, 567-588.
27
28 423 Cranford, P., Hargrave, B.T., Doucette, L.I., 2009. Benthic organic enrichment from
29
30 424 suspended mussel (*Mytilus edulis*) culture in Prince Edward Island, Canada. *Aquaculture*
31
32 425 292, 189-196.
33
34 426 Danovaro, R., Gambi, C., Luna, G.M., Mirto, S., 2004. Sustainable impact of mussel
35
36 427 farming in the Adriatic Sea (Mediterranean Sea): evidence from biochemical, microbial
37
38 428 and meiofaunal indicators. *Mar. Pollut. Bull.* 49, 325-333.
39
40 429 Filgueira, R., Grant, J., Bacher, C., Carreau, M., 2012. A physical-biogeochemical
41
42 430 coupling scheme for modeling marine coastal ecosystems. *Ecologic. Inform.* 7, 71-80.
43
44 431 Frechette, M., Grant, J., 1991. An in situ estimation of the effect of wind-driven
45
46 432 resuspension on the growth of the mussel *Mytilus edulis* L. *J. Exp. Mar. Biol. Ecol.* 148,
47
48 433 201-213.
49
50
51
52
53
54
55
56
57
58
59
60
61
62
63
64
65

- 1
2
3
4 434 Fugate, D.C., Friedrichs, C.T., 2003. Controls on suspended aggregate size in partially
5
6 435 mixed estuaries. *Estuar. Coast. Shelf. Sci.* 58, 389-404.
7
8
9 436 Gerdol, V., Hughes, R.G., 1994. Effect of *Corophium volutator* on the abundance of
10
11 437 benthic diatoms, bacteria and sediment stability in two estuaries in southeastern England.
12
13 438 *Mar. Ecol. Prog. Ser.* 114, 109-115.
14
15
16 439 Giles, H., Pilditch, C.A., 2004. Effects of diet on sinking rates and erosion thresholds of
17
18 440 mussel *Perna canaliculus* biodeposits. *Mar. Ecol. Prog. Ser.* 282, 205-219.
19
20
21 441 Giles, H, Broekhuizen, N., Byran, K.R., Pilditch, C.A., 2009. Modelling the dispersal of
22
23 442 biodeposits from mussel farms: The importance of simulating biodeposit erosion and
24
25 443 decay. *Aquaculture* 291, 168-178.
26
27
28 444 Gordon, N.D, McMahon, T.A., Finlayson, B.L, Gippel, C.J., Nathan, R.J., 2004. *Stream*
29
30 445 *Hydrology: An Introduction for Ecologists.* John Wiley and Sons, NJ. 254 p.
31
32
33 446 Grant, J., Gust, G., 1987. Prediction of coastal sediment stability from photopigment
34
35 447 content of mats of purple sulphur bacteria. *Nature* 330, 244-246.
36
37
38 448 Grant, J., Bathmann, U.V., Mills, E.L., 1986. The interaction between benthic diatom
39
40 449 films and sediment transport. *Estuar. Coast. Shelf. Sci.* 23, 225-238.
41
42
43 450 Grant, J., Walker, T.R., Hill, P.S., Lintern, D.G., 2013. BEAST-A portable device for
44
45 451 quantification of erosion in intact sediment cores. *Meth Oceanog.* 5, 39-55.
46
47
48 452 Grant, J., Curran, K.J., Guyondet, T.L., Tita, G., Bacher, C., Koutitonsky, V., 2007. A
49
50 453 box model of carrying capacity for suspended mussel aquaculture in Lagune de la
51
52 454 Grande-Entrée, Iles-de-la-Madeleine, Québec. *Ecol. Mod.* 200, 193-206.
53
54
55 455 Hartstein, N.D., Rowden, A.A., 2004. Effect of biodeposits from mussel culture on
56
57 456 macroinvertebrate assemblages at sites of different hydrodynamic regime. *Mar. Environ.*

1
2
3
4 457 Res. 57, 339-357.

5
6 458 Hatcher, A., Grant, J., Schofield, B., 1994. Effects of suspended mussel culture (*Mytilus*
7 spp.) on sedimentation, benthic respiration and sediment nutrient dynamics in a coastal
8 bay. Mar. Ecol. Prog. Ser. 115, 219-235.
9

10
11 461 Koutitonsky, V.G., Navarro, N., Booth, D., 2002. Descriptive physical oceanography of
12 Great-Entry Lagoon, Gulf of St. Lawrence. Estuar. Coastal Shelf Sci. 54, 833-847.
13

14 462 McKindsey, C.W., Archambault, P., Callier, M.D., Olivier, F., 2011. Influence of
15 suspended and off-bottom mussel culture on the sea bottom and benthic habitats: a
16 review. Can. J. Zool. 89, 622-646.
17

18 463 Miller, D.C., Norkko, A., Pilditch, C.A., 2002. Influence of diet on dispersal of horse
19 mussel *Atrina zelandica* biodeposits. Mar. Ecol. Prog. Ser. 242, 153-167.
20

21 464 Nickell, L.A., Black, K.D., Hughes, D.J., Overnell, J., Brand, T., Nickell, T.D., Breuer,
22 E., Harvey, S.M., 2003. Bioturbation, sediment fluxes and benthic community
23 structure around a salmon cage farm in Loch Creran, Scotland. J. Exp. Mar. Biol. Ecol.
24 285–286, 221-233.
25

26 465 Paterson, D.M., 1989. Short-term changes in the erodibility of intertidal cohesive
27 sediments related to the migratory behavior of epipelagic diatoms. Limnol. Oceanog. 34,
28 223-234.
29

30 466 Pearson, T.H., Rosenberg, R., 1978. Macrobenthic succession in relation to organic
31 enrichment and pollution of the marine environment. Oceanog. Mar. Biol. Ann. Rev. 16,
32 229-311.
33
34
35
36
37
38
39
40
41
42
43
44
45
46
47
48
49
50
51
52
53
54
55
56
57
58
59
60
61
62
63
64
65

- 1
2
3
4 478 Richard, M., Archambault, P., Thouzeau, G., Desrosiers, G., 2006. Influence of
5
6 479 suspended mussel lines on the biogeochemical fluxes in adjacent water in the Îles-de-la-
7
8 480 Madeleine (Quebec, Canada). *Can. J. Fish. Aquat. Sci.* 63, 1198-1213.
- 9
10
11 481 Richard, M., Archambault, P., Thouzeau, G., Desrosiers, G., 2007a. Summer influence of
12
13 482 1- and 2-yr-old mussel cultures on benthic fluxes in Grande-Entrée lagoon, Îles-de-la-
14
15 483 Madeleine (Québec, Canada). *Mar. Ecol. Prog. Ser.* 338, 131-143.
- 16
17
18 484 Richard, M., Archambault, P., Thouzeau, G., McKindsey, C.W., Desrosiers, G., 2007b.
19
20 485 Influence of suspended scallop cages and mussel lines on pelagic and benthic
21
22 486 biogeochemical fluxes in Havre-aux-Maisons lagoon, Îles-de-la-Madeleine (Quebec,
23
24 487 Canada). *Can. J. Fish. Aquat. Sci.* 64, 1491-1505.
- 25
26
27 488 Tolhurst, T.J., Black, K.S., Paterson, D.M., Mitchener, H.J., Termaat, G.R., Shayler, S.A.,
28
29 489 2000. A comparison and measurement standardization of four in situ devices for
30
31 490 determining the erosion shear stress of intertidal sediments. *Con. Shelf Res.* 20, 1397-
32
33 491 1418.
- 34
35
36 492 Tolhurst, T.J., Gust, G., Paterson, D.M., 2002. The influence of an extracellular polymeric
37
38 493 substance (EPS) on cohesive sediment stability. In: Winterwerp, J.C. Kranenburg, C.
39
40 494 (Eds.), *Fine Sediment Dynamics in the Marine Environment*. Elsevier Science,
41
42 495 Amsterdam. pp. 409-425
- 43
44
45 496 Walker, T.R., 2005. Vertical organic inputs and bioavailability of carbon in an Antarctic
46
47 497 coastal sediment. *Polish Pol. Res.* 26, 91-106.
- 48
49
50 498 Walker, T.R., Grant, J., 2009. Quantifying erosion rates and stability of bottom sediments
51
52 499 at mussel aquaculture sites in Prince Edward Island, Canada. *J. Mar. Syst.* 75, 46-55.
53
54
55
56
57
58
59
60
61
62
63
64
65

- 1
2
3
4 500 Walker, T.R., Grant, J., Cranford, P., Lintern, D.G., Hill, P.S., Jarvis, P., Barrel, J.,
5
6
7 501 Nozais, C., 2008. Suspended sediment and erosion dynamics in Kugmallit Bay and
8
9 502 Beaufort Sea during ice-free conditions. *J. Mar. Syst.* 74, 794-809.
10
11 503 Weise, A.M., Cromey, C.J., Callier, M.D., Archambault, P., Chamberlain, J., McKindsey,
12
13
14 504 C.W., 2009. Shellfish-DEPOMOD: Modelling the biodeposition from suspended shellfish
15
16 505 aquaculture and assessing benthic effects. *Aquaculture* 288, 239-253.
17
18
19 506 Widdows, J., Brinsley, M.D., Bowley, N., Barrett, C., 1998. A benthic annular flume for
20
21 507 in situ measurement of suspension feeding/biodeposition rates and erosion potential of
22
23
24 508 intertidal cohesive sediments. *Estuar. Coast. Shelf. Sci.* 46, 27-38.
25
26
27
28
29
30
31
32
33
34
35
36
37
38
39
40
41
42
43
44
45
46
47
48
49
50
51
52
53
54
55
56
57
58
59
60
61
62
63
64
65

Figure legends

Fig. 1. Mussel farm (grey rectangles) in Lagune de la Grande Entrée (LGE), Îles-de-la-Madeleine, Canada. Sampling stations distributed along a SW transect aligned with major current flow 0, 15 and 30 m from mussel farm. A reference station was located 500 m further along the transect.

Fig. 2. Sediment properties at LGE stations: (a) %TOC; (b) Proportion of mean sediment grain sizes. Silt and sand are sub-divided into very fine (vf), fine (f), medium (m), coarse (c), and very coarse (vc) fractions. D_{50} values (μm) are indicated; (c) %OM determined from a sub-sample of $<63 \mu\text{m}$ SPM collected and filtered through GF/F filters; (d) C:N ratios from 0-1cm sediment horizon. Significant differences determined by one-way ANOVA followed by Tukey's test; within each measured attribute, stations with same letters were not significantly different and stations with different letters were significantly different ($P<0.05$). Plotted values are means \pm SE ($n = 3$).

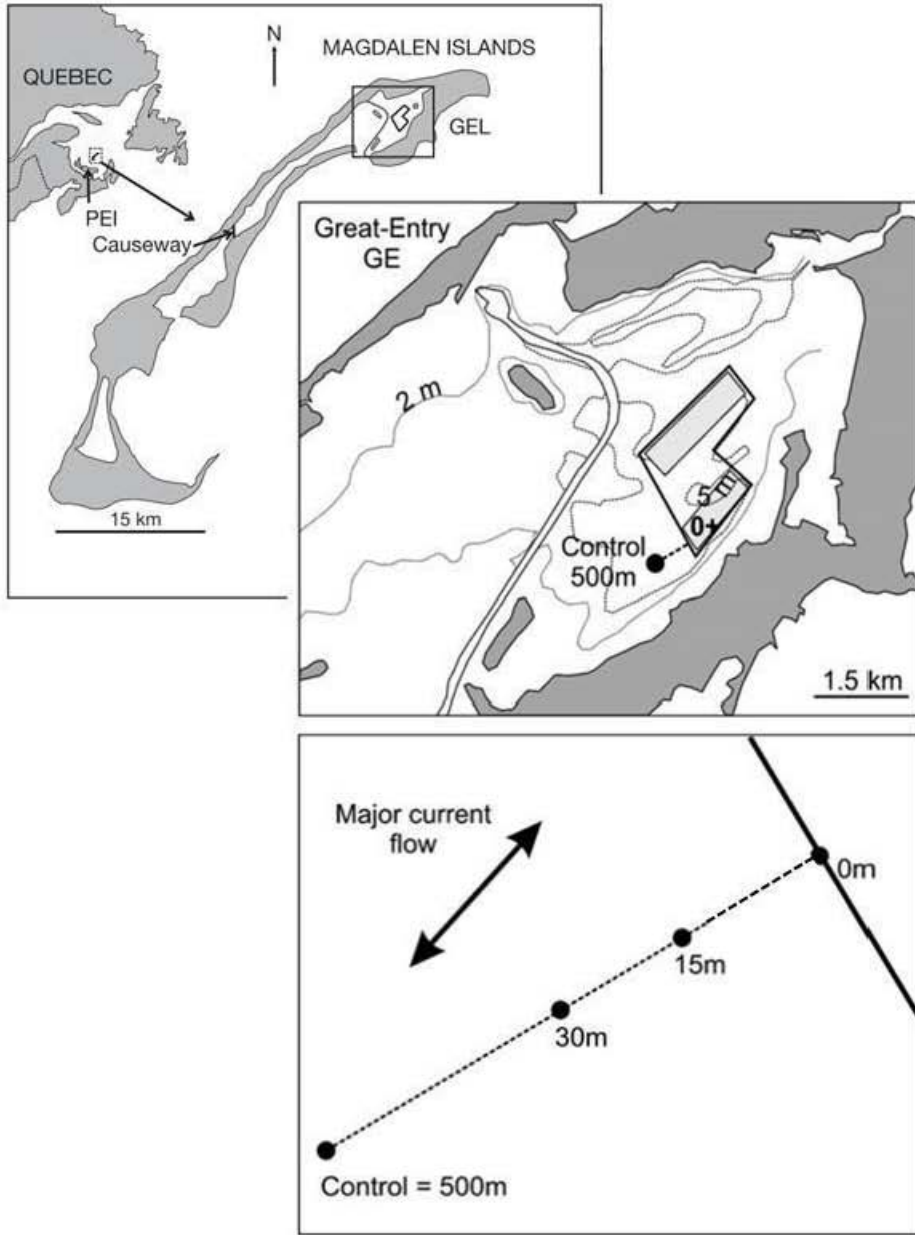
Fig. 3. Erosion sequences showing shear velocity (\circ), turbidity (% transmission) (\bullet) and erosion rate (grey circles) performed on sediment cores using the BEAST at increasing distances from a mussel line: (a) 0 m; (b) 15 m; (c) 30 m and (d) 500 m. Onset of erosion is indicated by vertical solid line (i.e., turbidity begins to increase). Onset of significant erosion (i.e., critical shear velocity) is indicated by the vertical dashed line which distinguishes between different phases of erosion.

Fig. 4. SPM concentrations at lowest % transmission (a); peak erosion rate (b); shear velocity at critical shear stress (u_{*crit}) (i.e., second phase of erosion) (c). Significant differences were determined by one-way ANOVA followed by Tukey's test; within each measured attribute, sites with same letters were not significantly different and sites with

1
2
3
4 different letters were significantly different ($P < 0.05$ for SPM concentrations) and
5
6 ($P < 0.10$ for erosion rate and shear velocity). Plotted values are means \pm S.E. ($n = 3$).
7
8

9 **Fig. 5.** Frequency of particle sizes (ESD, mm) resuspended from sediment cores under
10 different erosion thresholds. Sampling stations: 0, 15, 30 and 500 m subjected to u^*
11 between, 0.90-1.79 cm s^{-1} . Total number (n) of particles assessed at a given shear velocity
12 is indicated above each histogram.
13
14
15
16
17
18
19
20
21
22
23
24
25
26
27
28
29
30
31
32
33
34
35
36
37
38
39
40
41
42
43
44
45
46
47
48
49
50
51
52
53
54
55
56
57
58
59
60
61
62
63
64
65

Fig. 1.



1
2
3
4
5
6
7
8
9
10
11
12
13
14
15
16
17
18
19
20
21
22
23
24
25
26
27
28
29
30
31
32
33
34
35
36
37
38
39
40
41
42
43
44
45
46
47
48
49
50
51
52
53
54
55
56
57
58
59
60
61
62
63
64
65

Fig. 2.

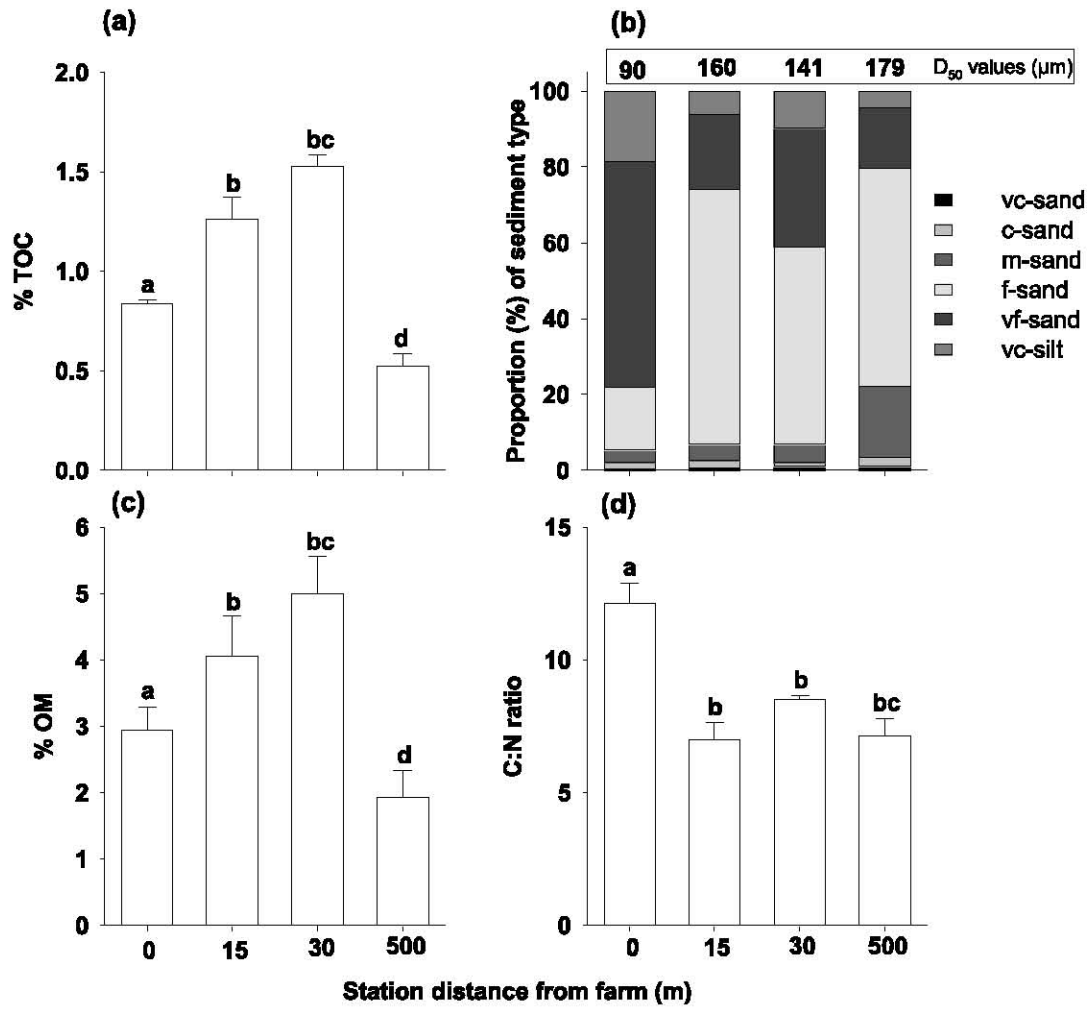


Fig. 3.

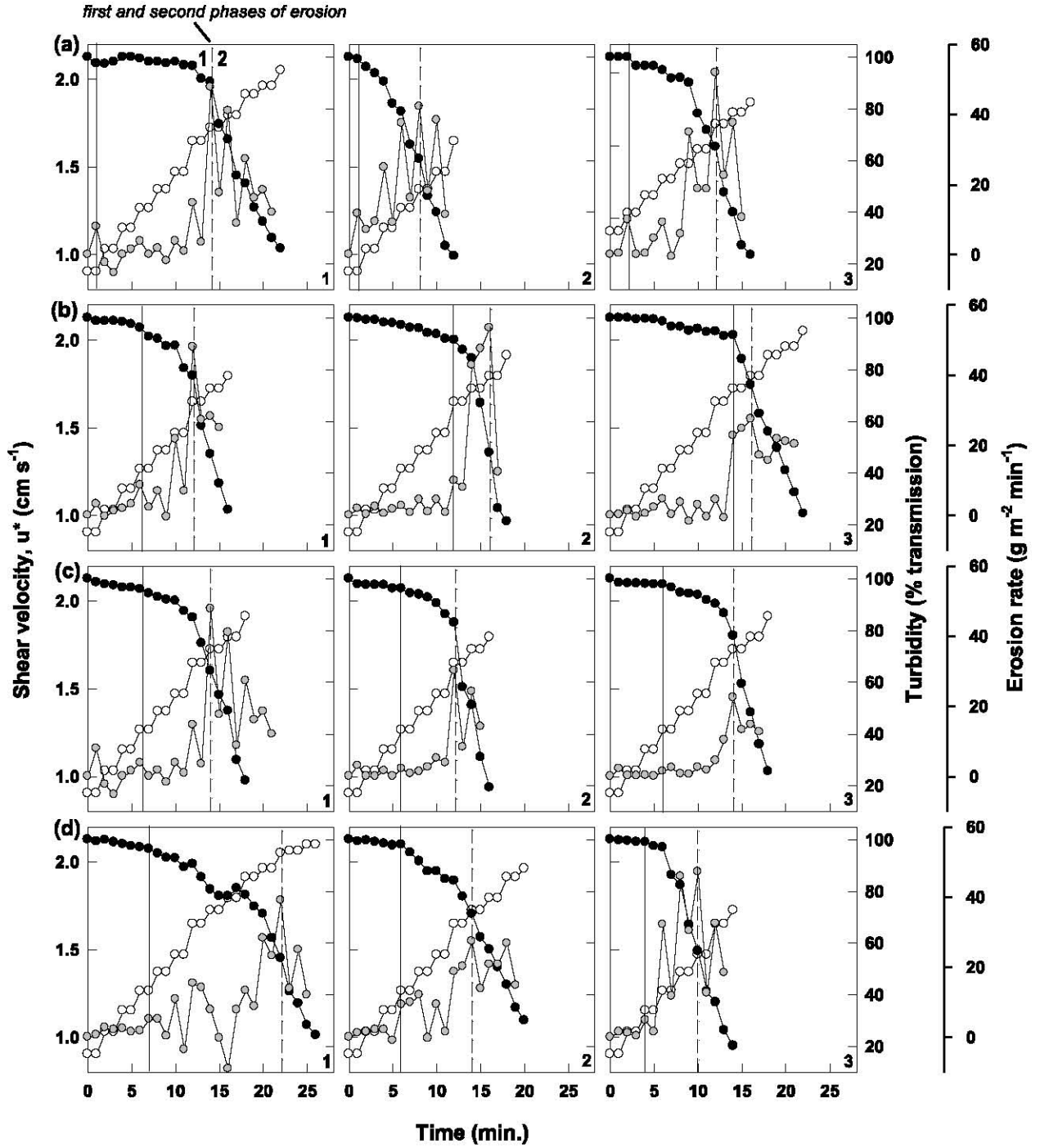


Fig. 4.

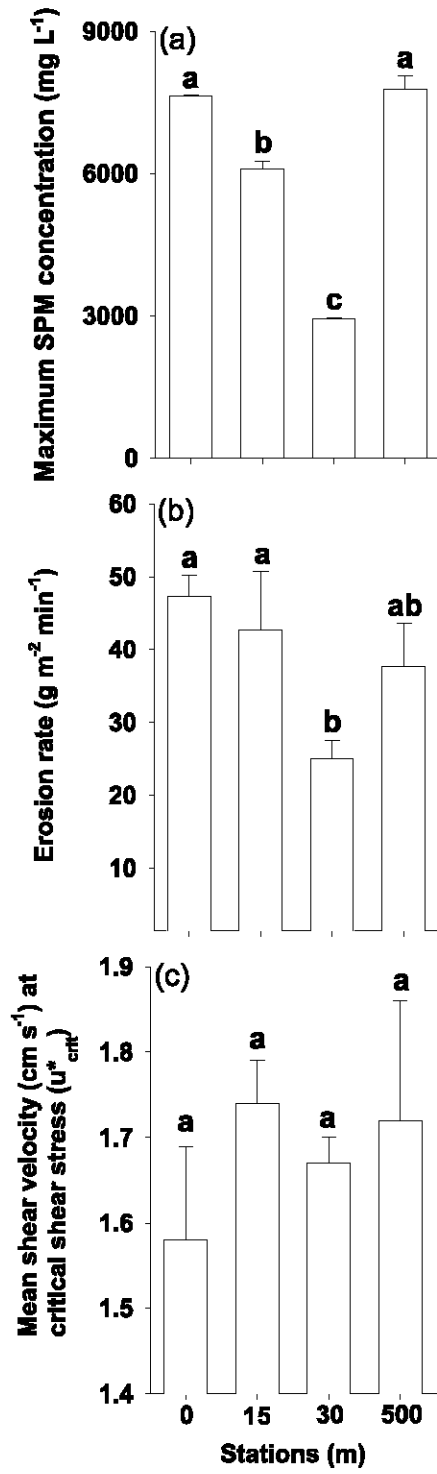


Fig. 5.

